JOURNAL OF APPLIED CRYSTALLOGRAPHY

ISSN: 1600-5767
journals.iucr.org/j

Algorithms for determining the phase of RHEED oscillations

Zbigniew Mitura and Sergei L. Dudarev

J. Appl. Cryst. (2015). **48**, 1927–1934

JOURNAL OF APPLIED CRYSTALLOGRAPHY

ISSN 1600-5767

Algorithms for determining the phase of RHEED oscillations

Zbigniew Mitura[a]* and Sergei L. Dudarev[b]

[a]Faculty of Metals Engineering and Industrial Computer Science, AGH University of Science and Technology, al. Mickiewicza 30, 30-059 Kraków, Poland, and [b]CCFE, Culham Science Centre, Oxfordshire OX14 3DB, UK. *Correspondence e-mail: mitura@metal.agh.edu.pl

Received 30 May 2015
Accepted 28 October 2015

Edited by S. Sasaki, Materials and Structures Laboratory, Tokyo Institute of Technology, Japan

Keywords: reflection high-energy electron diffraction (RHEED); RHEED oscillations; direct modelling; Fourier deconvolution.

Oscillations of reflection high-energy electron diffraction (RHEED) intensities are computed using dynamical diffraction theory. The phase of the oscillations is determined using two different approaches. In the first, direct, approach, the phase is determined by identifying the time needed to reach the second oscillation minimum. In the second approach, the phase is found using harmonic analysis. The two approaches are tested by applying them to oscillations simulated using dynamical diffraction theory. The phase of RHEED oscillations observed experimentally is also analysed. Experimental data on the variation of the phase as a function of the glancing angle of incidence, derived using the direct method, are compared with the values computed using both the direct and harmonic methods. For incident-beam azimuths corresponding to low-symmetry directions, both approaches produce similar results.

1. Introduction

Reflection high-energy electron diffraction (RHEED) is a robust and convenient technique for monitoring the growth of nanostructures at surfaces (Zdyb *et al.*, 2001; Sadowski *et al.*, 2007; Ohtake *et al.*, 2009; Krishnan *et al.*, 2010). Recently, it has been shown that RHEED measurements combined with the use of ultrafast lasers can be applied to the investigation of surface dynamics on femto- and picosecond time scales (Janzen *et al.*, 2006; Liang *et al.*, 2012). Quantitatively accurate methods for computing RHEED intensities, based on dynamical diffraction theory, were developed primarily for static singular flat surfaces (Ichimiya & Cohen, 2004; Peng *et al.*, 2004). Theoretical treatments were also generalized to include electron absorption and diffuse scattering by random configurations of atoms on a growing surface (Dudarev *et al.*, 1992, 1994; Dudarev, 1997).

RHEED became a broadly accepted practical tool for monitoring evolving surface structures after the discovery of the periodic intensity variation of electron beams reflected from a surface during crystal growth [Harris *et al.*, 1981; Wood, 1981; see also Herman & Sitter (1996) for more detail]. The period of such intensity variations, termed RHEED oscillations, corresponds to the deposition of one new monolayer onto a surface during growth. In the 1980s many experimental observations of RHEED oscillations were reported, describing conditions occurring during molecular beam epitaxial (MBE) growth of crystals, where experiments were performed in ultra-high vacuum. More recently, RHEED intensity oscillations were discovered at gas pressures considerably higher than the pressure characterizing molecular beam epitaxy conditions. For example, oscillations were observed during pulsed laser deposition (Rijnders *et al.*, 1997;

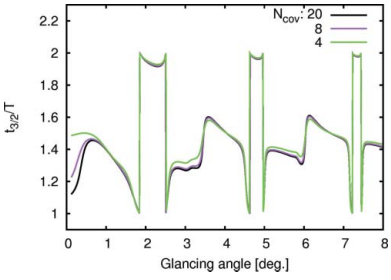

Li *et al.*, 2012). Several theoretical models for RHEED oscillations (Pukite *et al.*, 1988; Holmes *et al.*, 1997; Peng & Whelan, 1990) have been developed since the discovery of the effect, although the range of validity of these models remains limited. The subject has again attracted attention recently (Vasudevan *et al.*, 2014; Sullivan *et al.*, 2015).

In this paper we focus on algorithms for processing RHEED intensity oscillation data, and specifically on the determination of generic parameters characterizing the oscillations. For example, if we assume the availability of data describing some statistically representative oscillation data sets, we can characterize them by introducing parameters like the amplitude of the oscillations, their phase, the decay time constant *etc.* The values of such parameters can be determined by examining the oscillating intensity curves and matching the data to a chosen functional form. An alternative approach would be to use Fourier analysis, as this enables one to filter out fluctuations in the intensity oscillations. In general, interpreting intensity oscillations and analysing data proves quite complex. We focus here on the specific question of how to compare the phase of experimentally observed oscillations with that of oscillations predicted theoretically, assuming perfect layer-by-layer growth. RHEED oscillations observed experimentally are usually relatively smooth, as shown in Fig. 1, and their phase can be readily determined by identifying the interval of time to the intensity minimum during the second period of oscillations. However, curves computed using models based on dynamical diffraction theory often have a fairly complex shape, as illustrated in Fig. 2, and this is why it would be illuminating to compare the outcomes of analyses performed using a direct approach and a Fourier deconvolution method.

This work extends studies described by Mitura *et al.* (1998, 2002). In our earlier work, the phase of oscillations derived directly from experimental data was compared with the phase computed using dynamical diffraction theory and then analysed using the Fourier transform. In this study, we extract phase information from curves computed using dynamical diffraction theory, by applying two complementary approaches: first we identify the interval of time to the second minimum of oscillations, and then we perform harmonic analysis of the oscillations. Before proceeding to the interpretation of experimental data, we assess the advantages and disadvantages of both approaches. We also use a different model for crystal growth. Previously (Mitura *et al.*, 1998, 2002),

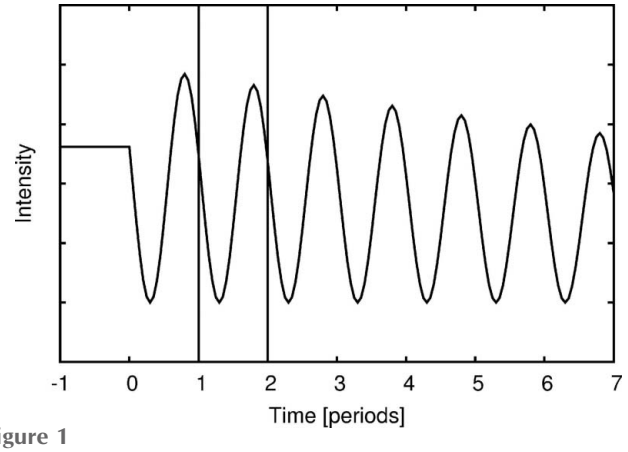

Figure 1
A typical example of the variation in RHEED intensity observed experimentally. Vertical lines are drawn for $t = T$ and $t = 2T$ to help identify the intensity variation over the second period of oscillations.

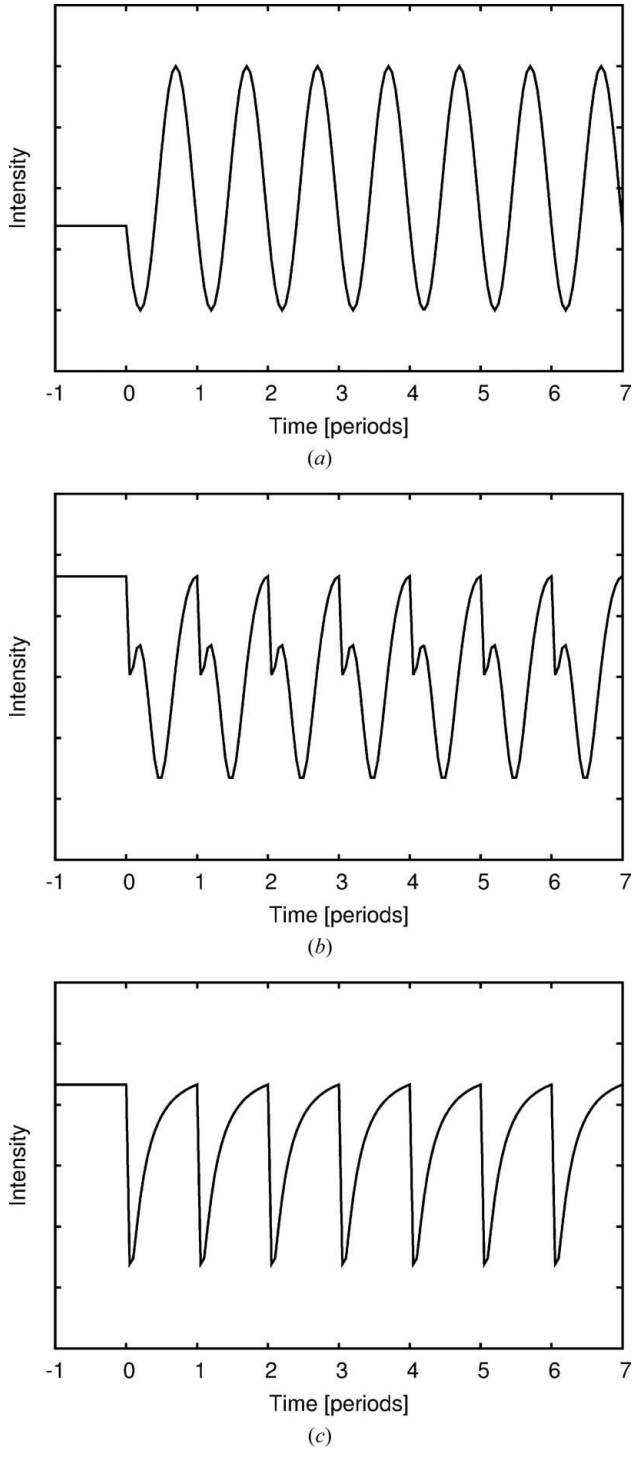

Figure 2
Examples of intensity oscillations used as input for the phase determination algorithms. (*a*) Oscillations resembling a cosine-like function. (*b*) Oscillations exhibiting double minima and maxima over a period. (*c*) Intensity changes that are strongly asymmetric over a period.

we assumed that the growing surface was reconstructed, but the positions of atoms at the surface were taken to be identical to those in the crystal bulk. Now, we start from a structural model ignoring surface reconstruction, but then, for the interpretation of experimental data, we use a model taking reconstruction into account, with the positions of Ga and As atoms at the surface being different from those in the bulk of the crystal. We also use a slightly different definition of the oscillation phase. In our earlier papers we assumed that the phase varied in the interval from $-\pi$ to π. Here, the values are in the range from 1 to 2, in agreement with the definition by Zhang *et al.* (1987) and Joyce *et al.* (1988).

The paper is organized as follows. In §2 we describe the two approaches to phase determination and apply them to the analysis of intensity oscillations predicted using dynamical diffraction theory. In §3 we analyse experimental observations, and in §4 we present our conclusions.

2. Two ways of determining the RHEED oscillation phase

We assume that, for any glancing angle of incidence, we can find the intensity of specular reflection by performing a dynamical diffraction calculation, as shown for example by Mitura *et al.* (1998, 2002) or Dudarev (1997). We are interested in analysing RHEED intensities for the azimuthal orientations of the incident beam that are off high-symmetry crystallographic directions. For such orientations, the intensity of the specular beam is almost insensitive to the lateral periodicity of the crystal surface. Hence, the effective potential describing the interaction between high-energy electrons and the crystal can be assumed to depend only on the coordinate in the direction normal to the surface (Dudarev *et al.*, 1992). This diffraction geometry is often referred to as the one-beam RHEED condition.

We assume that the electron–atom interaction potential in the growing layer is given by the potential of a complete atomic layer multiplied by the surface coverage Θ, where $0 < \Theta < 1$. For each glancing angle, the surface coverage varies on a mesh of values defined by the number of points $N_{\rm cov}$ for which, over one oscillation period, RHEED intensities are going to be computed. Over one oscillation period, the values of surface coverage for which we compute RHEED intensities are $\Theta = 0,\ 1/N_{\rm cov},\ 2/N_{\rm cov}, \ldots,\ (N_{\rm cov} - 1)/N_{\rm cov}$. Assuming perfect layer-by-layer growth, for each glancing angle we vary Θ and compute individual RHEED intensity *versus* time (*i.e.* intensity *versus* surface coverage) oscillation curves.

We investigated the growth of atomically thin GaAs layers on the (001) GaAs surface. The energy of the electrons was 10 keV. In this section, no surface reconstruction is assumed. Furthermore, the results described below refer to dynamical diffraction calculations, where the potential of interaction between the incident electrons and the atoms is evaluated ignoring thermal atomic vibrations. However, in §3 we use a detailed model of the (2×4) reconstruction, which takes thermal vibrations into account.

2.1. Direct determination of the phase

According to Zhang *et al.* (1987) and Joyce *et al.* (1988), the phase of oscillations can be defined as 'the time taken to reach the second oscillation minimum normalized by the time of a complete period'. The authors of the above papers introduced a symbol $t_{3/2}/T$ to denote the phase of oscillations defined in this way. For the cases illustrated in Figs. 1 and 2(*a*), this definition can be readily applied, and one expects that the phase would span the interval from 1 to 2. However, if multiple intensity minima occur over the second period of oscillations, as shown in Fig. 2(*b*), then the definition proposed by Zhang *et al.* (1987) becomes ambiguous. To make sure that the condition $1 \leq t_{3/2}/T < 2$ is satisfied even if the RHEED oscillations exhibit multiple minima over each oscillation period, we modify the definition given by Zhang *et al.* (1987). We define $t_{3/2}$ as the time corresponding to the lowest value of intensity over the second period of oscillations, and then define the oscillation phase by dividing the resulting value by the period of oscillations T. The phase computed in this way is denoted by $(t_{3/2}/T)_{\rm dir}$.

The use of the above definition for $(t_{3/2}/T)_{\rm dir}$ when interpreting experimentally observed oscillations does not cause any difficulty, as an oscillating intensity can be recorded as a continuous function of time. However, curves computed theoretically are somewhat more difficult to interpret, since they are computed on a discrete set of points where each point corresponds to a certain value of Θ.

The phase computed using the definition for $(t_{3/2}/T)_{\rm dir}$ given above is shown in Fig. 3. The plots were generated using several different values of $N_{\rm cov}$. Although in principle we are interested in the limit $N_{\rm cov} \rightarrow \infty$, the curve computed assuming $N_{\rm cov} = 20$ already provides a reasonably accurate approximation.

The phase of oscillations determined using the direct method is not a smooth function of the glancing angle, because the number of data points spanning the range of surface coverages Θ for which RHEED intensities are computed is finite, *i.e.* it equals $N_{\rm cov}$. Hence plots of the phase are discontinuous (Fig. 3). Still, in the limit of large $N_{\rm cov}$ the plot of

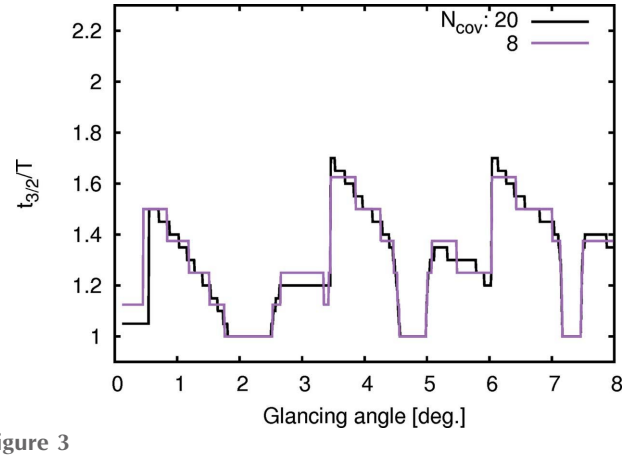

Figure 3
Plots of oscillation phase derived directly from the theoretical intensity oscillation curves computed for two values of $N_{\rm cov}$.

the phase becomes a smooth function. However, there is a reason why N_{cov} should not be taken as too large. The total calculation time required to determine the phase is proportional to N_{cov}, simply because N_{cov} different rocking curves, each corresponding to its own value of Θ, must be computed. In this paper, dynamical diffraction calculations are performed for the one-beam condition, and hence they are relatively fast. Under general many-beam RHEED diffraction conditions, a significantly longer computation time would be required, especially if diffuse scattering calculations were attempted using a supercell method. This is why, in practice, it is desirable to use a relatively modest number of points N_{cov} when performing dynamical diffraction simulations.

2.2. Determination of the phase using harmonic analysis

Whereas the algorithm for determining the phase directly from RHEED intensity curves described above may be successfully applied to simple cases, it would be desirable to introduce a more general definition of the oscillation phase, especially given that any experimentally observed curve involves small intensity fluctuations that need filtering out. This can be achieved using Fourier analysis. Any periodic function $f(t)$, where $f(t) = f(t + T)$ and T is the period, can be represented by a Fourier series as follows (Mitura *et al.*, 1998, 2002):

$$f(t) = \frac{A_0}{2} + A_1 \cos\left(\frac{2\pi t}{T} - \varphi_1\right) + \left[\sum_{n=2}^{\infty} A_n \cos\left(\frac{2\pi n t}{T} - \varphi_n\right)\right], \quad (1)$$

where we assume that $A_n \geq 0$ for $n \geq 1$. The terms corresponding to $n \geq 2$ can be filtered out and ignored. Since A_0 is a constant, we see that the general shape of the oscillations can be described by only two parameters, A_1 and φ_1. Appendix *A* shows how these two parameters can be found in practice.

We now compare values of phases derived from a direct examination of oscillations with those deduced using harmonic Fourier analysis. For oscillations with a simple cosine-like function shape, the values computed using the two approaches should be expected to agree well. To ensure this, we need to introduce a normalization convention. For example, we may compare values of φ_{dir}, defined as $\varphi_{dir} \equiv 2\pi[(t_{3/2}/T)_{dir} - 1.5]$, and φ_{harm}, defined as $\varphi_{harm} \equiv \varphi_1$ (Mitura *et al.*, 1998, 2002). In this study, we adopt a convention that matches the range of variation of the phase given by Zhang *et al.* (1987) and Joyce *et al.* (1988).

In what follows we assume that the phase $(t_{3/2}/T)_{dir}$ defined in §2.1 is equivalent to $(t_{3/2}/T)_{harm}$ defined as follows:

$$(t_{3/2}/T)_{harm} \equiv \frac{\varphi_1}{2\pi} + 1.5, \quad (2)$$

where φ_1 is the phase entering equation (1).

It is illuminating to see how the phase defined using Fourier analysis depends on the number of mesh points N_{cov} used in RHEED intensity calculations. Three plots of phase $(t_{3/2}/T)_{harm}$ computed using various values of N_{cov} are shown in Fig. 4. All of them are smooth and it appears that the plot computed for $N_{cov} = 8$ already approximates the limit $N_{cov} \rightarrow \infty$ fairly well.

2.3. Analysis of oscillations

In this section we compare phases of oscillations determined using the two methods described above. As a test, we apply the phase determination algorithms to the intensity oscillation curves computed theoretically using dynamical diffraction theory. To produce the curves shown in Fig. 5, we first compute RHEED intensity oscillation curves assuming an off-symmetry azimuth and using dynamical diffraction theory, as explained at the beginning of §2. Then, the phases of the oscillations are determined as described in §§2.1 and 2.2. In both cases, the number of mesh points N_{cov} used in the calculations when approximating surface coverage during growth is assumed to be 20. The incident angle step used in the calculations is 0.01°, although for clarity the plots in Fig. 5 only show points 0.05° apart.

Fig. 5 shows that the two plots are fairly similar, and they differ only over relatively narrow intervals of variation of the angle of incidence: from 1.9° to 2.5°, from 4.6° to 5.0°, and from 7.2° to 7.4°. We note that, despite the fact that over the

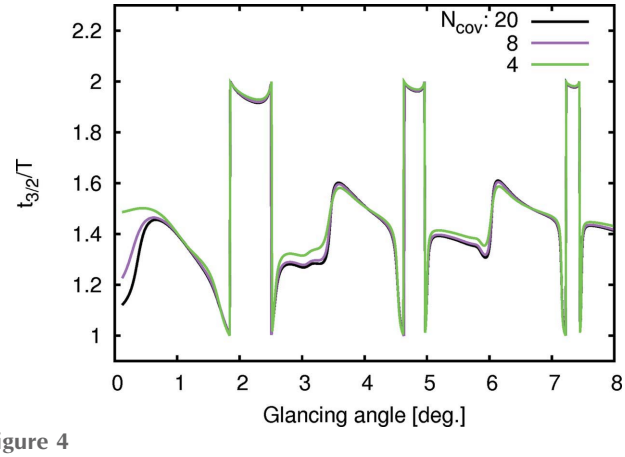

Figure 4
Plots of RHEED oscillation phase determined using harmonic analysis. The plots correspond to several different values of N_{cov}.

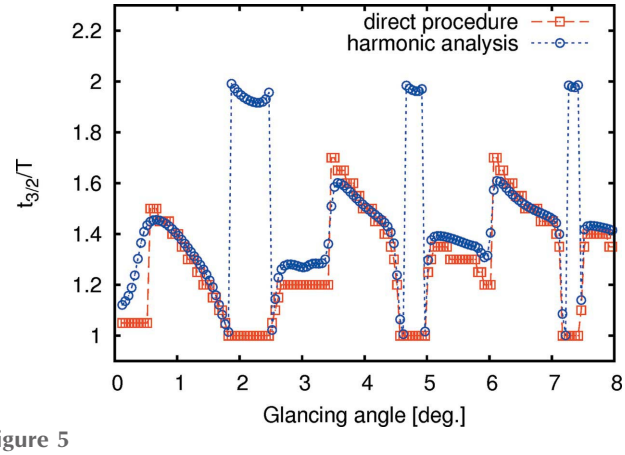

Figure 5
Plots of the oscillation phase determined using the two different approaches developed in this study (direct and employing a Fourier series) for identical intensity oscillation curves computed for $N_{cov} = 20$.

above intervals the values of the phase appear different, this difference is not materially significant since the phase only enters an expression for the observed intensity of the specular beam through an argument of a periodic function.

To clarify the point, we consider two sets of cosine-like oscillations that have the same period T, but are characterized by slightly different positions of the intensity minima. If we assume that the first set of oscillations has an intensity minimum at $t = 1.02T$, whereas the minimum of the second set is at $t = 0.99T$, we can say that the two sets are nearly identical. If we apply the direct method of phase determination to the two sets we discover that, for the first set, the value of the phase predicted by the direct method is 1.02, whereas the value of the phase derived from the second set is 1.99. The reason for the somewhat unexpectedly large value of the phase in the latter case is that the intensity minimum occurring during the first period of oscillations $t = 0.99T$ is not taken into account in the analysis. Physically there is no difference between the values of 0.99 or 1.99, and this example simply illustrates the point that a direct approach may produce discontinuous values if the phase is close to one of the boundaries of the interval [1, 2]. Furthermore, it can be shown that the phase determined using Fourier analysis exhibits the same characteristic behaviour.

From the examination of Fig. 5 we conclude that the plot of the phase derived using Fourier analysis is similar to the plot derived from a direct examination of the oscillations. In this study we focus on the development of algorithms for the determination of the phase and assume that RHEED oscillations can be described by a periodic function. In future it would be desirable to extend the treatment by taking the decay of the oscillations into account. For example, currently there is interest in developing a numerical treatment for analysing damped oscillations observed in mechanical spectroscopy measurements (Magalas & Majewski, 2009; Duda *et al.*, 2011; Tweten *et al.*, 2014). Developing models similar to those described above, but taking the decay of the oscillations into account, appears promising.

3. Interpretation of experimental data

In this section we focus on the interpretation of experimental data. The experimentally observed values of the phase of RHEED oscillations shown in Fig. 6 are taken from the literature (Crook *et al.*, 1989), where the values were determined by directly examining intensity oscillation data. The theoretical plots shown in Fig. 6 illustrate the dependence of the phases defined in §§2.1 and 2.2 on the angle of incidence.

It is appropriate to add a clarifying statement here. Ideally, it would be desirable to apply the two alternative methods of phase determination to *both* experimental and theoretical oscillation data, producing two plots of phase derived from experimental data, and two plots derived from simulations. Unfortunately, there is no detailed information available on the experimentally observed intensity oscillation curves described by Crook *et al.* (1989), so we are not able to apply the Fourier analysis method to experimentally observed oscillations. Still, we believe that it is useful to compare the two theoretical plots (obtained using the direct method and harmonic analysis) to identify the similarities and differences between the two methods.

The theoretical results displayed in Fig. 6 were produced assuming that the surface of the crystal was reconstructed as in the $\beta2(2 \times 4)$ model. For a review of models for reconstruction of the (001) GaAs surface, see Ohtake (2008). In our RHEED intensity simulations we used the two-As dimer model, where Ga atoms were absent in the missing dimer trenches (Chadi, 1987). We also assumed that, in the topmost layer, all the As atoms were displaced upwards (*i.e.* towards vacuum), that in the second layer the Ga atoms near the trenches were displaced downwards and, finally, that in the third layer two out of eight As atoms were displaced towards the crystal. The respective values of the atomic displacements were 0.05, −0.30 and −0.40 Å. In effect, we use here a simplified version of a more detailed model developed, using RHEED data, by Ohtake *et al.* (2002). Next, the Debye–Waller factors for both the As and Ga atoms were set to 2.0 Å^2. We also assumed a small delay associated with the start of MBE growth, similar to that used in the analysis by Osaka *et al.* (1995). Therefore, a constant value of 0.15 was added to all the initial values of the theoretically determined phases, *i.e.* to the phases found computationally using a perfect layer-by-layer model of MBE growth.

The examination of Fig. 6 shows that both theoretical plots agree well with the experimental observations. This suggests that our results are consistent with the detailed model for the structure of the GaAs(001)-(2 × 4) surface proposed by Ohtake *et al.* (2002). We also conclude that both methods for the determination of the phase of RHEED oscillations discussed above appear to be suitable for the interpretation of experimental data if the direction of incidence used for the RHEED observations satisfies the one-beam diffraction condition.

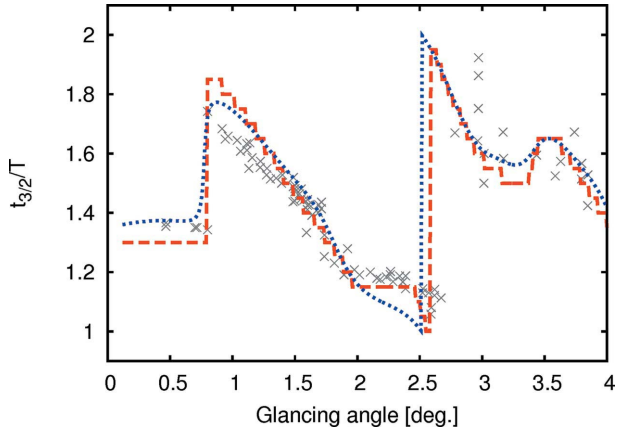

Figure 6
Comparison of experimental and theoretical phases of oscillations. Experimental data from Crook *et al.* (1989) are shown by crosses. The dashed line represents the theoretical results derived by direct examination of the oscillations, while the dotted line shows data derived using harmonic analysis of RHEED oscillations simulated using dynamical diffraction theory.

How does the analysis performed in this study relate to our earlier work (Mitura *et al.*, 1998, 2002)? When investigating RHEED oscillations, Mitura *et al.* (1998, 2002) assumed that the growing surface was reconstructed as in the $\beta2(2 \times 4)$ model, but all the atom positions were assumed to be the same as in a perfect crystal. The Debye–Waller factors were previously taken to be 2.05 and 1.90 Å^2 for the As and Ga atoms, respectively. Further, an additional imaginary part of the scattering potential was included in the treatment of RHEED to account for the loss of electrons resulting from scattering by step edges in the growing layer or by the atomic disorder on the growing surface (Dudarev *et al.*, 1992, 1994; Dudarev, 1997). In this study, to keep the treatment simple, we have omitted the imaginary part of the potential associated with atomic disorder (Dudarev *et al.*, 1992) and instead used a model where the imaginary part of the potential was proportional to its real part [see, for example, Dudarev *et al.* (1995)]. Next, we used the same values for the Debye–Waller factors of the As and Ga atoms. In a well known paper by Reid (1983), the values given for As are larger than those for Ga, but in a recent paper by Schowalter *et al.* (2009) an inverse ratio of the Debye–Waller factors was proposed. Both Reid (1983) and Schowalter *et al.* (2009) only considered the thermal vibrations of atoms in bulk crystals. Near a surface, the thermal displacements of atoms may be different from those in the crystal bulk. Again, to keep the treatment simple, we have assigned identical values of 2.0 Å^2 to the Debye–Waller factors of both As and Ga atoms.

Now we discuss the effect of surface reconstruction of the GaAs(001) surface. Present knowledge of this issue is more extensive than in the late 1990s. Then it was known that, under As-rich conditions, depending on the temperature of the sample, three different types of the (2×4) reconstruction may be observed, which were named, respectively, α, β and γ phases [see, for example, Hashizume *et al.* (1995)]. A number of surface atomic structure models were proposed to explain the experimental observations. An important question was raised about whether the three-As dimer model (called the β model) or the two-As dimer model (called the $\beta2$ model) gave the correct description of atomic positions in the β phase. In our previous work we used the $\beta2$ reconstruction model, where the positions of the atoms were assumed to be the same as in the crystal bulk (Mitura *et al.*, 1998, 2002). This is because the specific positions proposed by different authors were considered somewhat speculative at that time. At the moment the case appears a great deal clearer. Although research work, both experimental and theoretical, on the structure of the GaAs(001)-(2×4) surface is still ongoing (Debiossac *et al.*, 2014; Lin & Fichthorn, 2012), many fundamental questions have already been answered [see, for example, a recent review by Ohtake (2008)]. In brief, scanning tunnelling microscopy observations of well prepared surfaces have led to the conclusion that the three-As dimer model is not compatible with experimental data. Additionally, it was found that the α and γ phases of the (2×4) reconstruction can be regarded as disordered forms of the β phase. Altogether, it appears that the $\beta2$ model provides a fairly accurate representation of the fundamental structure of the GaAs(001)-(2×4) surface. If one ignores relatively minor points, it is possible to assume that, for each surface unit cell, two-As dimers are present in the topmost layer, and additionally, Ga atoms are absent from the atomic trenches. However, in general, the specific positions of the atoms should not be assumed to be identical to those in the bulk crystal structure. Hence, in this study we considered vertical displacements of some of the atoms (since in our RHEED calculations we use a one-dimensional scattering potential model not sensitive to displacements of the atoms parallel to the surface). The results (see Fig. 6) appear to be in better agreement with the experimental data than calculations performed previously.

There are further points that deserve mentioning. In the model adopted here we use only three adjustable parameters. This is appropriate, since the amount of information that can be derived from experimental observations is relatively limited. Also, we investigated the sensitivity of simulated RHEED intensities to the specific positions of atoms suggested by various authors. We found that the use of atomic positions derived from RHEED rocking curves by Ohtake *et al.* (2002) produced results similar to those where the atomic positions were derived from first-principles calculations (Schmidt & Bechstedt, 1996*a*,*b*; Ohtake *et al.*, 2002). The same can be said about the atomic positions derived from the analysis of X-ray scattering data (Garreau *et al.*, 1996; Ohtake *et al.*, 2002). In all the above cases, the theoretical calculations matched the experimental data fairly well. We also note that the directions of the atomic vertical displacements were the same in all the calculations, although the amplitudes of the displacements were different. If we used atom positions suggested by other authors, namely by Hashizume *et al.* (1995) or McCoy *et al.* (1998), the plots of the phase of RHEED oscillations derived from calculations did not agree well with experimental observations. According to Hashizume *et al.* (1995), the As atoms in the first layer are displaced downwards, whereas according to McCoy *et al.* (1998) the Ga atoms in the second layer are displaced upwards. Such atomic displacements do not agree with surface structure predictions derived by Schmidt & Bechstedt (1996*a*) from density functional theory. It appears that using a surface structure model consistent with the first-principles density functional calculations performed by Schmidt & Bechstedt (1996*a*) represents an important aspect of the theoretical treatment of RHEED oscillations essential for achieving agreement with experimental observations.

4. Conclusions

In this study we have compared phases of RHEED intensity oscillations derived from experimental observations using two alternative approaches to the determination of the phase of oscillations. We find that the phases determined using the two methods are in agreement with each other, although the results are not identical.

Determining the phase of oscillations directly is a good practical way of addressing the question if only a limited

amount of experimental information is available. However, the direct method becomes less efficient if a significant amount of data is available. Harmonic Fourier analysis may offer certain advantages in the latter case, particularly given that such analysis makes it possible to filter out fluctuations. In this paper, we have shown how to apply Fourier analysis to perfectly periodic oscillations, and have also shown that there is room for improving and generalizing the method, for example to the case of damped oscillations.

APPENDIX A
Determination of the phase using harmonic analysis

Here we explain how to find the values of A_1 and φ_1 used in equation (1). Let us assume that $f(t)$ is a periodic function of t, *i.e.* that $f(t) = f(t + T)$, where T is the period. Such a function can be represented by a Fourier series,

$$f(t) = \frac{C_0}{2} + \sum_{n=1}^{\infty}\left[C_n \cos\left(\frac{n2\pi t}{T}\right) + S_n \sin\left(\frac{n2\pi t}{T}\right)\right], \quad (3)$$

where

$$C_0 = \frac{2}{T}\int_0^T f(t)\,\mathrm{d}t, \quad (4)$$

and, for $n \geq 1$,

$$C_n = \frac{2}{T}\int_0^T f(t)\cos\left(\frac{n2\pi t}{T}\right)\mathrm{d}t, \quad (5)$$

$$S_n = \frac{2}{T}\int_0^T f(t)\sin\left(\frac{n2\pi t}{T}\right)\mathrm{d}t. \quad (6)$$

Using the trigonometric relation $\cos(\alpha - \beta) = \cos\alpha\cos\beta + \sin\alpha\sin\beta$, where α and β are real, we transform equation (1) as follows:

$$f(t) = \frac{A_0}{2} + \sum_{n=1}^{\infty}\left[A_n \cos\varphi_n \cos\left(\frac{n2\pi t}{T}\right) + A_n \sin\varphi_n \sin\left(\frac{n2\pi t}{T}\right)\right]. \quad (7)$$

Comparing terms in equations (3) and (7), we find that

$$A_0 = C_0, \quad (8)$$

and, for $n \geq 1$,

$$A_n \cos\varphi_n = C_n, \quad (9)$$

$$A_n \sin\varphi_n = S_n. \quad (10)$$

Using equations (9) and (10), we now derive formulae that enable us to compute A_1 and φ_1. In equation (1) it was assumed that $A_1 \geq 0$. Accordingly, A_1 satisfies the following condition

$$A_1 = \left(C_1^2 + S_1^2\right)^{1/2}. \quad (11)$$

Furthermore, since $A_1 > 0$, φ_1 can now be evaluated using the relation

$$\varphi_1 = \begin{cases} \arccos(C_1/A_1) & \text{if } S_1 > 0, \\ -\arccos(C_1/A_1) & \text{if } S_1 \leq 0. \end{cases} \quad (12)$$

It should be mentioned that, in the limit where $A_1 = 0$, the value of φ_1 is not defined, but encountering such a case in a practical calculation is not likely.

Equations (11) and (12) can be used to find A_1 and φ_1 if the values of C_1 and S_1 are known. The two latter quantities can be found using the following formulae:

$$C_1 \simeq \frac{2}{N_{\rm cov}}\sum_{l=0}^{N_{\rm cov}-1} f\left(\frac{lT}{N_{\rm cov}}\right)\cos\left(\frac{2\pi l}{N_{\rm cov}}\right), \quad (13)$$

$$S_1 \simeq \frac{2}{N_{\rm cov}}\sum_{l=0}^{N_{\rm cov}-1} f\left(\frac{lT}{N_{\rm cov}}\right)\sin\left(\frac{2\pi l}{N_{\rm cov}}\right). \quad (14)$$

Equations (13) and (14) are the approximate versions of equations (5) and (6). Specifically, equations (13) and (14) were derived assuming that $f(t)$ was defined on $N_{\rm cov}$ discrete points corresponding to a set of discrete time points t. Subsequently, l is an integer that varies from 0 up to $N_{\rm cov} - 1$. This parameter is also used when ordering the discrete time points.

The procedure described in this appendix applies to both theoretical and experimental oscillation data sets. We have shown how to apply it to oscillations computed theoretically. How does one apply the procedure to the analysis of experimental data? Further practical work is required to find an answer. However, it is already clear that data on regular oscillations spanning at least 20 periods are needed. One can then explore the second period, as in the direct method of phase determination. Consider the observed variation in intensity as a function of time $I(t)$, where t varies between T and $2T$, T being the period. In practice, the observed value of $I(T)$ may be slightly different from $I(2T)$. To comply with the mathematical definition of oscillations as a periodic function of time, the data may be corrected to ensure that the intensity curve has the same values at T and $2T$. The normalized intensity $I_{\rm norm}(t)$ can be defined as

$$I_{\rm norm}(t) = I(t) - [I(2T) - I(T)]\left(\frac{t - T}{T}\right). \quad (15)$$

For $I_{\rm norm}(t)$, we have

$$I_{\rm norm}(2T) = I_{\rm norm}(T). \quad (16)$$

Subsequently, the discrete values in equations (13) and (14) can be defined as

$$f\left(\frac{lT}{N_{\rm cov}}\right) = I_{\rm norm}\left(\frac{T + lT}{N_{\rm cov}}\right), \quad (17)$$

where l is again an integer that varies from 0 up to $N_{\rm cov} - 1$.

Acknowledgements

ZM gratefully acknowledges financial support of this work from the AGH, project No. 11.11.110.291. This work was

partly funded by the EUROfusion Consortium and received funding from the Euratom research and training programme 2014–2018 under grant agreement No. 633053, and from the RCUK Energy Programme (grant No. EP/I501045). The views and opinions expressed herein do not necessarily reflect those of the European Commission.

References

Chadi, D. J. (1987). *J. Vac. Sci. Technol. A*, **5**, 834–837.

Crook, G. E., Eyink, K. G., Campbell, A. C., Hinson, D. R. & Streetman, B. G. (1989). *J. Vac. Sci. Technol. A*, **7**, 2549–2553.

Debiossac, M., Zugarramurdi, A., Khemliche, H., Roncin, P., Borisov, A. G., Momeni, A., Atkinson, P., Eddrief, M., Finocchi, F. & Etgens, V. H. (2014). *Phys. Rev. B*, **90**, 155308.

Duda, K., Magalas, L. B., Majewski, M. & Zieliński, T. P. (2011). *IEEE Trans. Instrum. Meas.* **60**, 3608–3618.

Dudarev, S. L. (1997). *Micron*, **28**, 139–158.

Dudarev, S. L., Peng, L.-M. & Whelan, M. J. (1992). *Surf. Sci.* **279**, 380–394.

Dudarev, S. L., Peng, L.-M. & Whelan, M. J. (1995). *Surf. Sci.* **330**, 86–100.

Dudarev, S. L., Vvedensky, D. D. & Whelan, M. J. (1994). *Phys. Rev. B*, **50**, 14525–14538.

Garreau, Y., Sauvage-Simkin, M., Jedrecy, N., Pinchaux, R. & Veron, M. B. (1996). *Phys. Rev. B*, **54**, 17638–17646.

Harris, J. J., Joyce, B. A. & Dobson, P. J. (1981). *Surf. Sci.* **103**, L90–L96.

Hashizume, T., Xue, Q.-K., Ichimiya, A. & Sakurai, T. (1995). *Phys. Rev. B*, **51**, 4200–4212.

Herman, M. A. & Sitter, H. (1996). *Molecular Beam Epitaxy: Fundamentals and Current Status*, 2nd ed. Berlin, Heidelberg: Springer.

Holmes, D. M., Sudijono, J. L., McConville, C. F., Jones, T. S. & Joyce, B. A. (1997). *Surf. Sci.* **370**, L173–L178.

Ichimiya, A. & Cohen, P. I. (2004). *Reflection High-Energy Electron Diffraction.* Cambridge University Press.

Janzen, A., Krenzer, B., Zhou, P., von der Linde, D. & Horn-von Hoegen, M. (2006). *Surf. Sci.* **600**, 4094–4098.

Joyce, B. A., Zhang, J., Neave, J. H. & Dobson, P. J. (1988). *Appl. Phys. A*, **45**, 255–260.

Krishnan, R., Liu, Y., Gaire, C., Chen, L., Wang, G.-C. & Lu, T.-M. (2010). *Nanotechnology*, **21**, 325704.

Li, J., Peng, W., Chen, K., Zhang, Y., Cui, L. M., Chen, Y. F., Jin, Y. R., Zhang, Y. Z. & Zheng, D. N. (2012). *Solid State Commun.* **152**, 478–482.

Liang, W., Schäfer, S. & Zewail, A. H. (2012). *Chem. Phys. Lett.* **542**, 1–7.

Lin, Y. & Fichthorn, K. A. (2012). *Phys. Rev. B*, **86**, 165303.

Magalas, L. B. & Majewski, M. (2009). *Mater. Sci. Eng. A*, **521–522**, 384–388.

McCoy, J. M., Korte, U. & Maksym, P. A. (1998). *Surf. Sci.* **418**, 273–280.

Mitura, Z., Dudarev, S. L., Peng, L.-M., Gladyszewski, G. & Whelan, M. J. (2002). *J. Cryst. Growth*, **235**, 79–88.

Mitura, Z., Dudarev, S. L. & Whelan, M. J. (1998). *Phys. Rev. B*, **57**, 6309–6312.

Ohtake, A. (2008). *Surf. Sci. Rep.* **63**, 295–327.

Ohtake, A., Ozeki, M., Yasuda, T. & Hanada, T. (2002). *Phys. Rev. B*, **65**, 165315.

Ohtake, A., Yasuda, T. & Miyata, N. (2009). *Surf. Sci.* **603**, 826–830.

Osaka, J., Inoue, N. & Homma, Y. (1995). *Appl. Phys. Lett.* **66**, 2110–2112.

Peng, L.-M., Dudarev, S. L. & Whelan, M. J. (2004). *High-Energy Electron Diffraction and Microscopy*. Oxford University Press.

Peng, L.-M. & Whelan, M. J. (1990). *Surf. Sci.* **238**, L446–L452.

Pukite, P. R., Cohen, P. I. & Batra, S. (1988). In *Reflection High-Energy Electron Diffraction and Reflection Electron Imaging of Surfaces*, edited by P. K. Larsen & P. J. Dobson, pp. 427–447. New York: Plenum Press.

Reid, J. S. (1983). *Acta Cryst.* A**39**, 1–13.

Rijnders, G. J. H. M., Koster, G., Blank, D. H. A. & Rogalla, H. (1997). *Appl. Phys. Lett.* **70**, 1888–1890.

Sadowski, J., Dłużewski, P., Kret, S., Janik, E., Łusakowska, E., Kanski, J., Presz, A., Terki, F., Charar, S. & Tang, D. (2007). *Nano Lett.* **7**, 2724–2728.

Schmidt, W. G. & Bechstedt, F. (1996*a*). *Surf. Sci.* **360**, L473–L477.

Schmidt, W. G. & Bechstedt, F. (1996*b*). *Phys. Rev. B*, **54**, 16742–16748.

Schowalter, M., Rosenauer, A., Titantah, J. T. & Lamoen, D. (2009). *Acta Cryst.* A**65**, 5–17.

Sullivan, M. C., Ward, M. J., Gutiérrez-Llorente, A., Adler, E. R., Joress, H., Woll, A. & Brock, J. D. (2015). *Appl. Phys. Lett.* **106**, 031604.

Tweten, D. J., Ballard, Z. & Mann, B. P. (2014). *J. Sound Vib.* **333**, 2804–2811.

Vasudevan, R. K., Tselev, A., Baddorf, A. P. & Kalinin, S. V. (2014). *ACS Nano*, **8**, 10899–10908.

Wood, C. E. C. (1981). *Surf. Sci.* **108**, L441–L443.

Zdyb, R., Stróżak, M. & Jałochowski, M. (2001). *Vacuum*, **63**, 107–112.

Zhang, J., Neave, J. H., Dobson, P. J. & Joyce, B. A. (1987). *Appl. Phys. A*, **42**, 317–326.